

New Relativistic Particle-In-Cell Simulation Studies of Prompt and Early Afterglows from GRBs

K.-I. Nishikawa^{*}, J. Niemiec[†], H. Sol^{**}, M. Medvedev[‡], B. Zhang[§], Å. Nordlund[¶], J. Frederiksen[¶], P. Hardee^{||}, Y. Mizuno^{*}, D. H. Hartmann^{††} and G. J. Fishman^{‡‡}

^{*}National Space Science and Technology Center, Huntsville, AL 35805

[†]Institute of Nuclear Physics PAN, ul. Radzikowskiego 152, 31-342 Kraków, Poland

^{**}LUTH, Observatoire de Paris-Meudon, 5 place Jules Jansen, 92195 Meudon Cedex, France

[‡]Department of Physics and Astronomy, University of Kansas, KS 66045, USA

[§]Department of Physics, University of Nevada, Las Vegas, NV 89154, USA

[¶]Niels Bohr Institute, University of Copenhagen, Juliane Maries Vej 30, 2100 Copenhagen Ø, Denmark

^{||}Department of Physics and Astronomy, The University of Alabama, Tuscaloosa, AL 35487

^{††}Clemson University, Clemson, SC 29634-0978, USA

^{‡‡}NASA/MSFC, Huntsville, AL 35805

Abstract. Nonthermal radiation observed from astrophysical systems containing relativistic jets and shocks, e.g., gamma-ray bursts (GRBs), active galactic nuclei (AGNs), and microquasars commonly exhibit power-law emission spectra. Recent PIC simulations of relativistic electron-ion (or electron-positron) jets injected into a stationary medium show that particle acceleration occurs within the downstream jet. In collisionless, relativistic shocks, particle (electron, positron, and ion) acceleration is due to plasma waves and their associated instabilities (e.g., the Weibel (filamentation) instability) created in the shock region. The simulations show that the Weibel instability is responsible for generating and amplifying highly non-uniform, small-scale magnetic fields. These fields contribute to the electron's transverse deflection behind the jet head. The resulting "jitter" radiation from deflected electrons has different properties compared to synchrotron radiation, which assumes a uniform magnetic field. Jitter radiation may be important for understanding the complex time evolution and/or spectra in gamma-ray bursts, relativistic jets in general, and supernova remnants.

Keywords: Weibel instability, magnetic field generation, radiation

PACS: Relativistic Particle-In-Cell Simulation, Studies of Prompt and Early Afterglows from GRBs

INTRODUCTION

Shocks are believed to be responsible for prompt emission from gamma-ray bursts (GRBs) and their afterglows, for variable emission from blazars, and for particle acceleration processes in jets from active galactic nuclei (AGN) and supernova remnants (SNRs). The predominant contribution to the observed emission spectra is often assumed to be synchrotron- and inverse Compton radiation from these accelerated particles [15, 21]. It is assumed that turbulent magnetic fields in the shock region lead to Fermi acceleration, producing higher energy particles [2, 1]. To make progress in understanding emission from these object classes, it is essential to place modeling efforts on a firm physical basis. This requires studies of the microphysics of the shock process in a self-consistent manner [16, 19].

New Numerical Method for Calculating Emission

The retarded electric field from a charged particle moving with instantaneous velocity β under acceleration $\dot{\beta}$ is obtained [7, 12, 13, 14]. After some calculation and

simplifying assumptions the total energy W radiated per unit solid angle per unit frequency can be expressed as

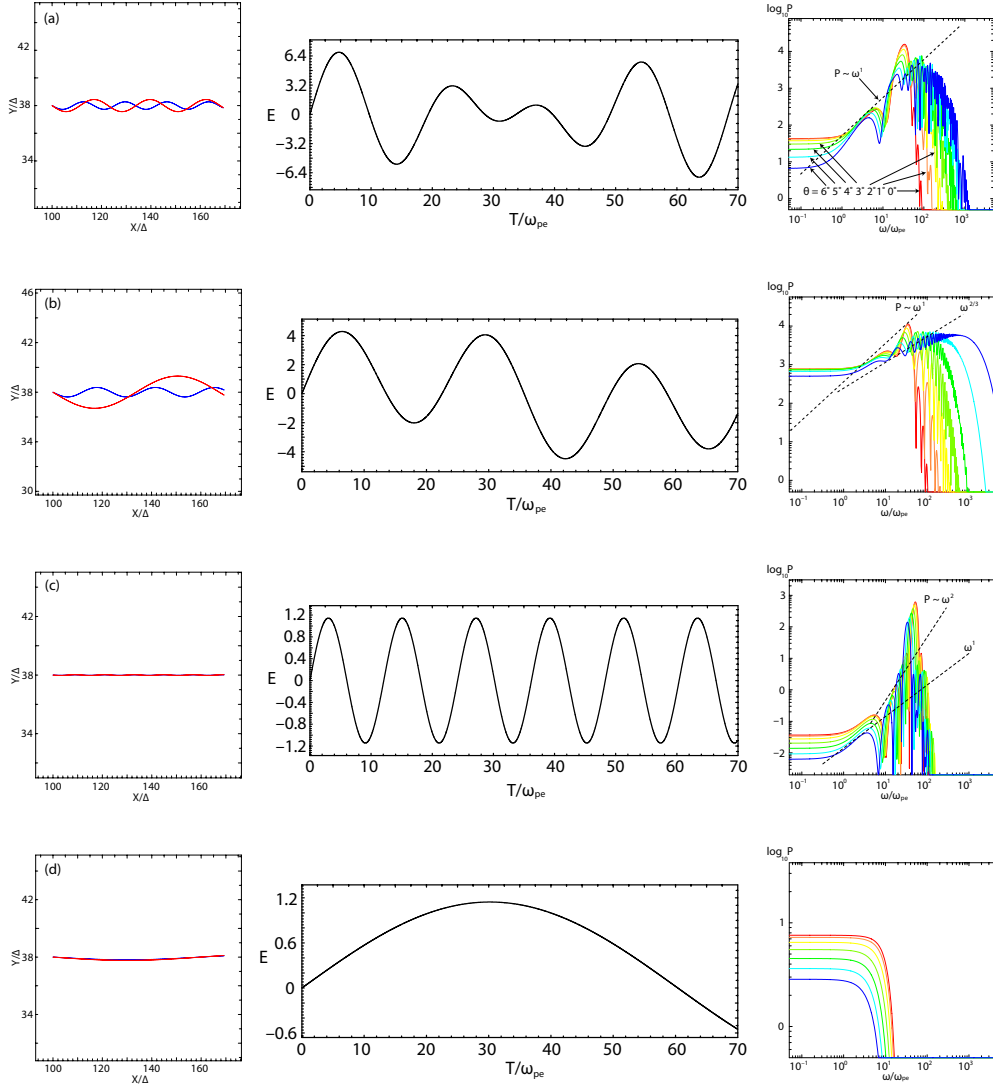
$$\frac{d^2W}{d\Omega d\omega} = \quad (1)$$

$$\frac{\mu_0 c q^2}{16\pi^3} \left| \int_{-\infty}^{\infty} \frac{\mathbf{n} \times [(\mathbf{n} - \beta) \times \dot{\beta}]}{(1 - \beta \cdot \mathbf{n})^2} e^{i\omega(t' - \mathbf{n} \cdot \mathbf{r}_0(t')/c)} dt' \right|^2$$

Here, $\mathbf{n} \equiv \mathbf{R}(t')/|\mathbf{R}(t')|$ is a unit vector that points from the particle's retarded position towards the observer. The first term on the right hand side, containing the velocity field, is the Coulomb field from a charge moving without influence from external forces in eq. 2.4 [4]. The second term is a correction term that arises when the charge is subject to acceleration. Since the velocity-dependent field falls off in distance as R^{-2} , while the acceleration-dependent field scales as R^{-1} , the latter becomes dominant when observing the charge at large distances ($R \gg 1$). The choice of unit vector \mathbf{n} along the direction of propagation of the jet (hereafter taken to be the x -axis) corresponds to head-on emission. For any other choice of \mathbf{n} (e.g., $\theta = 1/\gamma$), off-axis emission is seen by the observer. The observer's viewing angle is set by the choice of \mathbf{n} ($n_x^2 + n_y^2 + n_z^2 = 1$).

TABLE 1. Seven cases of radiation

	B_x	$V_{j1,2}$	$V_{\perp,1}$	$V_{\perp,2}$	γ_{\max}	θ_{Γ}	Remarks
P	3.70 (B_z)	0.0c	0.998c	0.9997c	40.08	4.491	gyrating
A	3.70	0.99c	0.1c	0.12c	13.48	13.35	jet
B	3.70	0.9924c	0.1c	0.12c	36.70	4.905	jet
C	3.70	0.99c	0.01c	0.012c	7.114	25.30	jet
D	0.370	0.99c	0.01c	0.012c	7.114	25.30	jet
E	0.370	0.99c	0.1c	0.12c	13.48	13.35	$\Delta t = 0.005$
F	0.370	0.99c	0.1c	0.12c	13.48	13.35	$\Delta t = 0.025$



RADIATION FROM TWO ELECTRONS

In the previous section we discussed how to obtain the retarded electric field from relativistically moving particles (electrons) observed at large distance. Using eq. 1 we calculated the time evolution of the retarded electric field and the spectrum from a gyrating electron in a uni-

form magnetic field to verify the technique used in this calculation. We have calculated the radiation from two electrons gyrating in the $x - y$ plane in the uniform magnetic field B_z with Lorentz factors ($\gamma = 15.8, 40.8$) (Case P in Table 1) [12, 13, 14]. We have very good agreement between the spectrum obtained from the simulation and the theoretical synchrotron spectrum expectation from

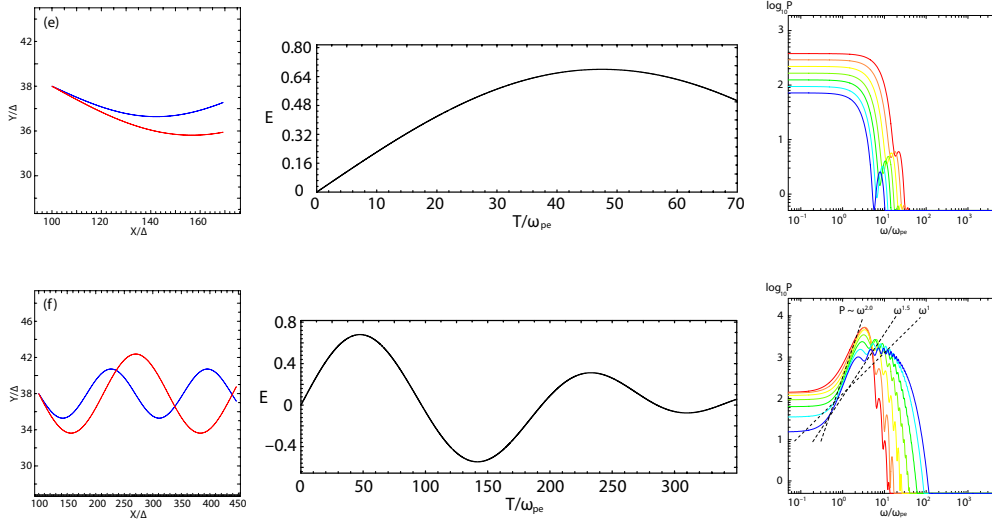


FIGURE 1. Summary of six cases with jet velocity (Cases A - F) (for Case P, see Nishikawa et al. [14])

eq. 7.10 [5].

In order to calculate more realistic radiation from relativistic jets we included a parallel magnetic field (B_x). Relativistic jets are propagating along the x direction. Table 1 shows six cases including the previous case P (first row) [14]. The jet velocity is $0.99c$ (except Case B). Two different magnetic field strengths are used. Two electrons are injected with two different perpendicular velocities (Cases A - F). The maximum Lorentz factors, $\gamma_{\max} = \{(1 - (V_{j2}^2 + V_{\perp 2}^2)/c^2)\}^{-1/2}$ are calculated for larger perpendicular velocity. The critical angles for the off-axis radiation is calculated with $\theta_{\Gamma} = \Gamma^{-1}$.

Figure 1 shows the summary of the six cases. Trajectories of the two electrons are shown in the left column (red: larger perpendicular velocity, blue: smaller perpendicular velocity). The two electrons propagate from left to right with gyration in the $y-z$ plane (not shown). The gyroradius is about 0.44Δ ($\Delta = 1$: the simulation grid length) for the electron with a larger perpendicular velocity (Case A). The radiation electric field from the two electrons is shown in the middle column. The spectra were calculated at the point $(x, y, z) = (64,000,000.0, 43.0, 43.0)$ shown in the right column. The seven curves show the spectrum at the viewing angles 0° (red), 1° (orange), 2° (yellow), 3° (moss green), 4° (green), 5° (light blue), and 6° (blue) ($n_y \neq 0$). The higher frequencies become stronger with the increasing viewing angle. For Case A the power spectrum is scaled as $P \sim \omega^1$ as proposed for jitter radiation [8]. For all Cases the spectra are much steeper than the slope $1/3$ for the synchrotron radiation.

The second row in Fig. 1 shows Case B with a larger jet velocity $V_{j1,2} = 0.9924c$ with the other parameters kept the same as Case A. The spectra with larger view-

ing angles are similar to those of Case A. The spectrum slope is smaller than that in Case A. However, due to the large jet velocity the higher frequencies at larger viewing angles ($0^\circ, 1^\circ, 2^\circ$) become stronger. On the other hand, with the smaller perpendicular velocities (Cases C and D), the gyroradius becomes very small. The spectra become weaker than those in Case A. As shown in the third and fourth rows in Fig. 1, the viewing angle dependence becomes very small. It should be noted that the slope of spectra is very steep for Case C. Spectral leakage is found.

Cases D - F have a weaker magnetic fields ($B_x = 0.370$) than Cases A - C. Case D has a small perpendicular velocity. The trajectories are almost straight. The spectra look very similar to that for Bremsstrahlung [5]. The spectra become flat at lower frequencies. The peak spectral power is the weakest of all the cases. With larger perpendicular velocities the spectra become stronger than those with the smaller perpendicular velocities. Case F shows the case with a larger time step (5 times) with the same parameters as Case E. The spectrum slope is very steep. The spectra in this case show two differences with those in Case E. First there exist positive slopes in the lower frequency. Second, due to the gyro-motion the spectra split due to the viewing angles. In particular the spectrum with larger viewing angle becomes stronger at high frequencies.

As shown in Table 1, the critical angles for the off-axis radiation $\theta_{\Gamma} = \Gamma^{-1}$ are different. In this study we have obtained the off-axis radiation for the angles $0^\circ, 1^\circ, 2^\circ, 3^\circ, 4^\circ, 5^\circ$, and 6° ($n_y \neq 0$). For cases D, E, and F the variation among different viewing angles is small since the angles are much smaller than the critical angle (25.3° and 13.35°). However, for case B ($\theta_{\Gamma} = 5^\circ$) the

radiation shows larger differences for different viewing angles due to the small critical angle. For Case F (a longer time $(340/\omega_{pe})$) the spectra at high frequencies become stronger with larger viewing angles.

These results validate the technique used in our code. It should be noted that the method based on the integration of the retarded electric fields calculated by tracing many electrons described in the previous section can provide a proper spectrum in turbulent electromagnetic fields. On the other hand, if the formula for the frequency spectrum of radiation emitted by a relativistic charged particle in instantaneous circular motion is used [7, 18], the complex particle accelerations and trajectories are not properly accounted for and the jitter radiation spectrum is not properly obtained.

DISCUSSION

The procedure used to calculate jitter radiation using the technique described in the previous section has been implemented in our code.

In order to obtain the spectrum of synchrotron (jitter) emission [9, 8, 3], we consider an ensemble of electrons randomly selected in the region where the filamentation (Weibel) instability [20] has fully developed, and electrons are accelerated in the generated magnetic fields. We calculate emission from about 20,000 electrons during the sampling time, $t_s = t_2 - t_1$ with Nyquist frequency $\omega_N = 1/2\Delta t$ where Δt is the simulation time step and the frequency resolution $\Delta\omega = 1/t_s$. However, since the emission coordinate frame for each particle is different, we accumulate radiation at fixed angles in simulation system coordinates after transforming from the individual particle emission coordinate frame. This provides an intensity spectrum as a function of angle relative to the simulation frame x -axis (this can be any angle by changing the unit vector \mathbf{n} in eq. (1)). A hypothetical observer in the ambient medium (viewing the external GRB shock) views emission along the system x -axis. This computation is carried out in the reference frame of the ambient medium in the numerical simulation. For an observer located outside the direction of bulk motion of the ambient medium, e.g., internal jet shocks in an ambient medium moving with respect to the observer, an additional Lorentz transformation would be needed along the line of sight to the observer. Spectra obtained from simulations can be rescaled to physical time scales.

Emission obtained by the method described above is self-consistent, and automatically accounts for magnetic field structures on the small scales responsible for jitter emission. By performing such calculations for simulations with different parameters, we can then investigate and compare the quite contrasted regimes of jitter- and synchrotron-type emission [9, 8, 3] for prompt and afterglow emission. The feasibility of this approach has been

demonstrated and implemented [6, 5]. Thus, we will be able to address the issue of low frequency GRB spectral index violation of the synchrotron line of death [8].

Simulations incorporating jitter radiation are in progress using an MPI code [11] which speeds up considerably from the previous OpenMP code [17]. New results of jitter radiation will be presented separately.

ACKNOWLEDGMENTS

We have benefited from many useful discussions with A. J. van der Horst. This work is supported by AST-0506719, AST-0506666, NASA-NNG05GK73G and NNX07AJ88G. JN was supported by MNiSW research projects 1 P03D 003 29 and N N203 393034, and The Foundation for Polish Science through the HOMING program, which is supported through the EEA Financial Mechanism. Simulations were performed at the Columbia facility at the NASA Advanced Supercomputing (NAS). Part of this work was done while K.-I. N. was visiting the Niels Bohr Institute. He thanks the director of the institution for generous hospitality.

REFERENCES

1. Blandford, R. & Eichler, D. 1987, Phys. Rep., 154, 1
2. Fermi, E. 1949, Phys. Rev. 75, 1169
3. Fleishman, G. D. 2006, ApJ, 638, 348
4. Hededal, C.B., 2005, PhD thesis (arXiv:astro-ph/0506559)
5. Hededal, C. B. and Nishikawa, K.-I. 2005, ApJ, 623, L89
6. Hededal, C.B., & Nordlund, Å. 2005, submitted to ApJL (arXiv:astro-ph/0511662)
7. Jackson, J. D. 1999, *Classical Electrodynamics*, Interscience
8. Medvedev, M. V. 2006, ApJ, 637, 869
9. Medvedev, M. V. 2000, ApJ, 540, 704
10. Medvedev, M.V. & Loeb, A. 1999, ApJ, 526, 697
11. Niemiec, J., Pohl, M., Stroman, T. & Nishikawa, K.-I. 2008, ApJ, 684, 1174
12. Nishikawa, K.-I., Mizuno, Y., Fishman, G. J., & Hardee, P., 2008a, (arXiv:0801.4390)
13. Nishikawa, K.-I., Hardee, P., Mizuno, Y., Medvedev, M., Zhang, B., Hartmann, D. H., & Fishman, G. J. 2008b, (arXiv:0802.2558)
14. Nishikawa, K. -I., Mizuno, Y., Hardee, P., Sol, H., Medvedev, M., Zhang, B., Nordlund, A., Frederiksen, J. T., Fishman, G. J. & Preece, R. 2008c, published in for the Proceedings of Science of the Workshop on Blazar Variability across the Electromagnetic Spectrum, April 22 to 25, 2008 (arXiv:0808.3781)
15. Piran, T. 2005a, Rev. Mod. Phys. 76, 1143
16. Piran, T. 2005b, in the proceedings of Magnetic Fields in the Universe, Angra dos Reis, Brazil, Nov. 29-Dec 3, 2004, Ed. E. de Gouveia del Pino, (arXiv:astro-ph/0503060)
17. Ramirez-Ruiz, E., Nishikawa, K.-I., & Hededal, C. B., 2007, ApJ, 671, 1877
18. Rybicki, G. B., & Lightman, A. P. 1979, *Radiative Processes in Astrophysics*, John Wiley & Sons, New York
19. Waxman, E. 2006, Plasma Phys. Control. Fusion, 48 B137
20. Weibel, E. S. 1959, Phys. Rev. Lett., 2, 83
21. Zhang, B. 2007, Chin. J. Astron. Astrophys. 7, 1